PHYSICAL REVIEW B VOLUME 17, NUMBER 10 15 MAY 1978

Interpretation of angle-resolved x-ray photoemission spectra

Michael J. Sayers and F. R. McFeely
Department of Chemistry, Research Laboratory of Electronics, Massachusetts Institute of Technology, Cambridge, Massachusetts 02139
(Received 18 October 1977)

This paper presents several new considerations concerning angle-resolved x-ray photoemission. Phonon-assisted processes are explicitly considered; it is found that even when such processes dominate direct transitions, agreement between theoretical predictions and experiment is obtained only if the final states are treated as Bloch-like and highly mixed. The use of augmented-plane-wave final states and a proper statistical treatment of the x-ray photon field is outlined for copper and found to yield nearly quantitative agreement with experimental results. The relationship between this and older plane-wave model calculations is discussed in detail, as is the physical significance of the new results.

I. INTRODUCTION

Recently, a great deal of research and controversy has centered about angle-resolved x-ray-photoemission-spectra (ARXPS) measurements of the valence-band spectra of the noble metals. Following the initial observation by Baird *et al.*[1] that the ARXPS of the gold valence bands showed distinctly different shapes depending upon the direction of photoelectron propagation, two conflicting theories were proposed. Baird, Wagner, and Fadley argued that the anisotropies arise from the severe constraints of wave-vector conservation with the matrix elements for the photoionization process contributing negligibly to the anisotropy. The alternative theory was given by McFeely *et al.*,[2] who argued that plane-wave mixing in the final states made wave-vector conservation unimportant in determing the shape of the spectra. They argued instead that the dipole matrix elements for the photoionization process exhibited angular anisotropies and calculated these anisotropies based upon the assumption of plane-wave final states. In particular, they noted that in spectra collected from photoelectrons propagating along {111} axes, only the t_{2g}-type d-band states had nonzero matrix elements; for spectra obtained along {100} axes, only e_g character was active. It was therefore asserted by the authors that these experiments provided a direct measure of the t_{2g} and e_g projections of the d-band density of states. Wehner *et al.*[3] compared the two theories for the case of the Cu(001) surface and found that the plane-wave matrix-element model of McFeely *et al.* gave excellent agreement with experiments for five out of six spectra. Relatively poor agreement was obtained for the [001] propagation direction, which we shall see was both significant and systematic.

It has recently been demonstrated, both theoretically and experimentally, that due to thermal disorder the number of direct wave-vector-conserving transitions in these spectra is negligible. Thus, the angle dependence of the dipole matrix elements must be responsible for the spectral variations.

For these effects to be spectroscopically useful (as opposed to nuisances precluding straightforward spectral analysis), it is necessary that a model be developed that explains the spectra quantitatively and in detail. In this paper we present calculations which accomplish this task. These calculations show that *none* of the angle-resolved spectra of the noble metals hitherto reported in the literature represents a pure t_{2g} or e_g partial density of states, and that a good deal of the apparent success of the original plane-wave model applied to Cu by Wehner *et al.* and Apai *et al.*[4] is due to cancellation of errors. We also demonstrate the importance of the explicit inclusion of the photon polarization effects in order to explain the details of the spectra.

In Sec. II, we describe the theoretical basis of our calculations. These calculations are then compared with experiment and with the earlier plane-wave calculations in Sec. III. General conclusions concerning these methods are given in Sec. IV.

II. THEORETICAL DISCUSSION

A. Role of phonons and the final-state manifold

As has been pointed out by Shevchik[5] and indicated in experiments by Williams *et al.*,[6] the assumption of a direct-transition model in the x-ray-photoemission-spectra (XPS) regime is generally invalid. A simple Debye treatment of the oscillation of Cu atoms about their equilibrium positions reveals that for a photon energy of 1487 eV, roughly 95% of all transitions fail to conserve momen-

tum. A thoroughgoing atomic-scale treatment of vibrations in solids shows that such transitions may be considered as phonon-assisted processes. We begin therefore by exploring the nature of such processes; for simplicity, only one-phonon processes will be considered for the moment.

Indirect transitions can be considered as two-step processes. Consequently, second-order time-dependent perturbation theory, which explicitly connects initial and final states through virtual intermediate levels, is appropriate. We may write the perturbing Hamiltonian for the coupled photon-phonon system

$$H'(\vec{r},t)=\tfrac{1}{2}A^{\omega}(\vec{r})(e^{i\omega t}+e^{-i\omega t}) + \tfrac{1}{2}V^{q}(r)(e^{i\omega_q t}+e^{-i\omega_q t}), \quad (1)$$

where ω and $A^{\omega}(\vec{r})$ characterize the photon absorption, and $V^{q}(\vec{r})$ and ω_q characterize the phonon scattering. Following methods given, for example, by Wooten,[7] we get the result for the transition rate between initial state $|0\rangle$ and final state $|f\rangle$ that

$$W_{f0}=\frac{2\pi}{\hbar}\delta(E_{f0}-h\omega\pm h\omega_q)\left(\frac{|V^{q}_{fi}|^2|A^{\omega}_{i0}|^2}{(\omega_{i0}-\omega)^2} + \frac{|V^{q}_{i'0}|^2|A^{\omega}_{fi'}|^2}{(\omega_{fi'}-\omega)^2}\right). \quad (2)$$

The first term in the brackets corresponds to an "off-resonance" photoabsorption from $|0\rangle$ to an intermediate state $|i\rangle$ followed by phonon scattering from $|i\rangle$ into the final state; an equivalent process corresponding to the second term is the photoabsorption from a second "intermediate" state $|i'\rangle$ to $|f\rangle$, followed by scattering of the hole at $|i'\rangle$ back to $|0\rangle$.

Due to the high photon energies and angular resolution involved in the ARXPS experiment, the formidable form Eq. (2) is considerably simplified. Equation (2) shows that an accurate prediction of spectral angular dependence depends on accurate photon matrix elements, which in turn entails the use of correct final-state wave functions. A good first choice for this purpose would be a superposition of augmented plane waves (APW's); these functions adequately represent the wave function in the atomic cores which dominate the photoexcitation step. Thus,

$$|f\rangle=\sum_{\vec{G}} a_{\vec{G}}(\vec{k})\,|\mathrm{APW}(\vec{k}+\vec{G})\rangle. \quad (3)$$

This function describes a set of partial waves, each propagating in the direction $\vec{k}+\vec{G}$. Of these, the angular resolution of our experiments selects only one partial-wave component (and those parallel to it). Moreover, within the range of $\vec{G}$'s important to $|f\rangle$, variations in $|G|$ are unimportant; these constraints enable one to calculate the required photon matrix element using a very small set of $\vec{G}$'s, and this element will depend only upon the direction of propagation and the relative availability of the final state as manifested in the coefficient $a_{\vec{G}}(\vec{k})$.

We now must consider the nature of the final states described by Eq. (3). This is a result of the factors $(\Delta E)^{-2}$ in the transition rate (2), which could lead to appreciable sensitivity of the spectrum to the density of final states. We consider as illustration the consequences of Eq. (2) under two previous models which had some success in explaining angle-resolved x-ray photoemission spectra.

Baird, Wagner, and Fadley[1] proposed a final-state manifold which is completely free-electron-like in nature. This constraint coupled with that of restricting transitions to be energy conserving and "direct" allows transitions from only a small "disk" of states in the first Brillouin zone (BZ), the location of this disk, as a function of photoelectron propagation direction being the determinant of the spectral angular dependence.

One might suppose that the coupling of phonon and electron momenta would automatically scramble the sampling of $\vec{k}$ states and allow transition from the entire first BZ to a given final state. Nonetheless, nondirect transitions would be strongly suppressed to a degree leaving the disk model intact. In the XPS experiment, a typical value of $|G|$ is $\sim 12(2\pi/a)$ and the resulting change in energy across a band is $(13^2-11^2)\,(2\pi/a)^2 \simeq 50$ Ry. The factors $(\Delta E)^{-2}$ in Eq. (2) consequently suppress transitions other than those very nearly vertical (i.e., nearly direct), and one would be left with Brillouin-zone selective photoemission due to a resonance enhancement. This result is not paradoxical in relation to Shevchik's in that his result indicated the fraction of direct and indirect transitions involved, and said nothing of how "nonvertical" transitions must be.

The second term of Eq. (2) involving phonon scattering from $|0\rangle$ to $|i'\rangle$ and photoabsorption from $|i'\rangle$ to $|f\rangle$ does not alter this conclusion. Since the phonon-scattering process is isoergic to within a few meV, an indirect process occurs only if $|0\rangle$ and $|i'\rangle$ are degenerate. Therefore, the disk of states giving BZ selective photoemission can be mapped into a new set of states $|0\rangle$ which give rise to spectral features *identical* to those of the $|i'\rangle$ disk. Therefore, the constraints of energy conservation and free-electron dispersion relation *alone* are sufficient to generate disk-model effects. The difficulties encountered in predicting angular dependences have been docu-

mented by Wehner *et al.*,[3] and suggest that the free-electron curve yields a seriously inaccurate final density of states.

We adopt then a viewpoint similar to that of McFeely *et al.*[2] These authors argue that the crystal potential strongly mixes partial waves of nearly the same direction. This destroys any simple energy–photoelectron-momentum relation and so gives rise to sampling throughout the first BZ. The theoretical grounds discussed by the original authors, and the more recent evidence of the failure of the disk model forms the basis for our adoption of this viewpoint.

Our approach to the high-energy photoemission process may then be termed a "statistical" one. Based on simple models of the phonon-electron interaction,[8] we assume the phonon matrix elements V_{if}^{q} to be isotropic and of equal magnitude at the energies involved; their role is to permit transitions from any point in the first BZ to any given final momentum. The high density of states resulting from partial-wave mixing moreover allows us to assume that all transitions have an equal likelihood of being "on-resonance" and of propagating in a detectable direction. The problem of calculating the transition rate to a given energy and momentum then reduces to a calculation of a photon matrix element between valence-band states and an "average" final-state wave function. As was seen above, this function is of the form of one (or a few) partial-wave components of an APW.

Lastly, one must be concerned with the consequences of calculating matrix elements for *intermediate* states as opposed to the final state. On the scale of electronic energy bands, phonons are essentially dispersionless; their effect can be to perturb the propagation direction of the photoelectron from that of the intermediate to the final state. Since the matrix elements are slow functions of angle, it is sufficient to show that the intermediate and final states do not correspond to propagation in significantly different directions.

We may now remove a restriction employed earlier and treat N phonon processes; that is, processes in which N phonons, each uncorrelated with the others, combine to give a resultant phonon to which the electron couples. The question of interest then is what is the average angle between an intermediate state (of wave vector $\vec{G}$) and a final state (of wave vector $\vec{G}+\vec{Q}$). The average angle between $|\vec{Q}|_{\rm rms}$ and $\vec{G}$ is 57°, and so we have

$$\tan\theta_{\rm rms} = |Q|_{\rm rms}\sin(57^\circ)/[|G| + |Q|_{\rm rms}\cos(57^\circ)]\,. \tag{4}$$

The relation between $|Q|_{\rm rms}$ and $|q|_{\rm rms}$, where q corresponds to a one-phonon process, may be treated as a three-dimensional random-walk problem with variable step-length distribution. The absence of correlation between steps gives us in general

$$\langle Q^2\rangle = \langle N\rangle q^2\,. \tag{5}$$

Employing a spherical-BZ approximation (i.e., a Debye model) gives a probability distribution in the magnitude of q

$$P(q)\,dq = \begin{cases} 0, & q > q_D \\ \dfrac{3q^2\,dq}{q_{\rm D}^3}, & q \le q_D\,, \quad q_D = \left(\dfrac{24\pi^2}{a^3}\right)^{1/3}, \end{cases} \tag{6}$$

where q_D is the familiar Debye cutoff value. Putting Eq. (6) into Eq. (5), taking $|G| = 12$, and inserting these results into Eq. (4) gives the result

$$\tan(\theta)_{\rm rms} = 0.622\sqrt{N}/(12\sqrt{3} + 0.44\sqrt{N})\,. \tag{7}$$

For N as high as 4, the value of $\theta_{\rm rms}$ does not exceed 3.5°, which is essentially the angle of spectrometer acceptance. Even for the unreasonably high value $N = 10$, the angular dispersion is only slightly in excess of 5°. Thus, there is a slight "blurring" of the angular distribution, but one which is entirely insignificant in its effects.

B. Calculation of the matrix elements

The matrix-element calculations presented here differ in two fundamental ways from the earlier work of McFeely *et al.*[2] and Apai *et al.*[4] First, more accurate final-state wave functions are employed, and second, a proper statistical treatment of the impinging electromagnetic field is made. Both of these points will be seen to be important to a proper quantitative understanding of the spectra.

The evaluation of $\langle f|\nabla|i\rangle$ was effected by employing the customary dipole approximation. Consistent with our statistical approach, the final-state partial APW which propagates into the detector is assumed to have a constant amplitude independent of the initial states. The initial states themselves are treated in the modified tight-binding scheme previously employed by McFeely *et al.*[2] and Apai *et al.*[4] and, as in the previous work, only the d-band components of the states are explicitly considered. The matrix element was factorized into radial and angular parts. The radial factors were treated numerically in the acceleration representation $\langle r\rangle \sim \langle -\nabla V(r)\rangle_{fi}$, where $V(r)$ is the self-consistent muffin-tin potential of an atom in the lattice. $V(\vec{r})$ was calculated by an $X\alpha$–self-consistent-field (SCF) method ($\alpha = 1$) and placed in a Herman-Skillman mesh. The potential was used

as input to a program which numerically integrates the Schrödinger equation, the algorithm being based on the Runge-Kutta-Gill method. The same potential was used for both initial and final states; the energies at which the integrations were performed were the SCF d-orbital energy for the initial state, and 1487 eV for the final state. $(\nabla V)_r$ was then estimated at each point of the integration, and the element $\langle -\nabla V(r)\rangle_{fi}$ approximated as the sum

$$(-\nabla V)_{fi} = -\sum_{r_i} \psi_{\text{fin}}(l, E_f, r_i)\nabla V(r_i) \times \psi_{\text{init}}(l', E_i, r_i) r_i^2 \Delta r_i , \tag{8}$$

where ψ_{fin} and ψ_{in} are the final- and initial-state wave function, respectively. The mesh typically had ~500 points between $r = 0.0005$ a.u. and the muffin-tin radius, where the integration was terminated. The angular factors were treated after a method outlined by Gadzuk,[9] and reduced in essence to a sum of Gaunt coefficients multiplied by spherical harmonics in momentum space, the sum running over all m values consistent with dipole-allowed final-state p- and f-channel transitions.

Taking the values of ∇_{if} as determined, then, one is left with the problem of evaluating the square of the term $\hat{\epsilon}\cdot\nabla_{if}$. Previous approaches simply called $\hat{\epsilon}$ a scalar constant for simplicity on the grounds that the radiation was unpolarized. However, this "simplification" is the physical equivalent of assuming the radiation is *polarized*, with polarization vector given by

$$\hat{\epsilon} = (1/\sqrt{3})(\hat{x} + \hat{y} + \hat{z}) . \tag{9}$$

This is certainly incorrect, and, as we shall show, can lead to serious errors. The x-ray source is sufficiently beamlike that it will have a well-defined propagation vector $\vec{q}_{h\nu}$ in the crystal frame; as a transverse field, the x radiation will have no component along this beam. Use of Eq. (9) as a representation of this state of affairs is generally inappropriate to light other than that polarized along the $\{111\}$ direction. Rather, one should take an ensemble average of $(\hat{\epsilon}\cdot\nabla_{if})^2$ and then sum this value over all symmetry-related degenerate states in the other irreducible parts of the BZ. When this is done, the final form of the matrix element is given by

$$|V_{if}|^2 = 16\sigma_{t_{2g}} \sum_{i=1}^{3}\sum_{\alpha,\beta} (d_i^\alpha)^*(d_i^\beta)\langle \epsilon_\alpha \epsilon_\beta\rangle + 24\sigma_{e_g} \sum_{i=4}^{5}\sum_{\alpha,\beta} (d_i^\alpha)^*(d_i^\beta)\langle \epsilon_\alpha \epsilon_\beta\rangle . \tag{10}$$

Here d_i $(i = 1, \ldots, 5)$ corresponds to matrix elements for d_{xy}, d_{yz}, d_{xz}, $d_{x^2-y^2}$, and d_{z^2}, respectively; $\alpha, \beta = x$, y, or z; and $\sigma_{e_g} = |C_4|^2 + |C_5|^2$, $\sigma_{t_{2g}} = |C_1|^2 + |C_2|^2 + |C_3|^2$, where the C_i are coefficients of the d orbitals determined in the tight-binding form for $|i\rangle$.

This leaves the "polarization matrix" (effectively, the density matrix of the photons) to be evaluated. For unpolarized light, this is trivially done by writing the electromagnetic vectors $\vec{E}$ and $\vec{H}$ as monochromatic plane waves, e.g.,

$$\vec{E} = E_0\, \hat{e} \exp[i(\vec{q}_{h\nu}\cdot\vec{r} - \omega t)] , \qquad \vec{H} = \vec{H}_0 \exp[i(\vec{q}_{h\nu}\cdot\vec{r} - \omega t)] . \tag{11}$$

A straightforward evaluation of Maxwell's equations for $\nabla\times\vec{E}$ and $\nabla\times\vec{H}$ then leads to the result

$$\vec{E} = (\tilde{1} - \hat{q}_{h\nu}\otimes\hat{q}_{h\nu})\vec{E} , \tag{12}$$

where $\hat{q}_{h\nu}$ is the unit propagation vector of $\vec{E}$, $\tilde{1}$ is a unit matrix, and $\otimes$ denotes an outer product. Noting that

$$\langle \epsilon_\alpha \epsilon_\beta\rangle = \langle E_\alpha E_\beta\rangle / |E|^2 , \tag{13}$$

and replacing the ensemble average by a time average, in which the polarization vector may be considered to rotate sinusoidally about the axis $\hat{q}$, we arrive at the final result

$$\langle \epsilon_\alpha \epsilon_\beta\rangle = \tfrac{1}{2}(\delta_{\alpha\beta} - \hat{q}_{h\nu}^{(\alpha)}\hat{q}_{h\nu}^{(\beta)}) , \tag{14}$$

where $\delta_{\alpha\beta}$ is the Kronecker delta.

For polarized light, of course, the matrix component $\langle \epsilon_\alpha \epsilon_\beta\rangle$ is given as the product of the α and β components of the polarization vector.

III. COMPARISON WITH EXPERIMENT

The results of the statistical final-state model developed above have been calculated for photoemission along the [001] and [111] directions from copper, and compared with the high-resolution angle-resolved XPS results of Apai *et al.*[4] These ARXPS results of Apai *et al.*[4] These directions were chosen because of the high resolution of these experiments and because the simpler plane-wave matrix-element theory of McFeely *et al.*,[2] suggests that these spectra should show maximal dissimilarity. Therefore, a model capable of predicting both spectra accurately should probably be capable of predicting less extreme cases as well.

Much of the following discussion concerns the superiority of the representation of the final state as a single APW component over that of a plane wave. As has been noted by Shevchik,[10] a plane-wave function does not possess the proper symmetry in the vicintiy of the atomic cores, where photoabsorption occurs. In consequence, he suggests that APW's should be superior to some de-

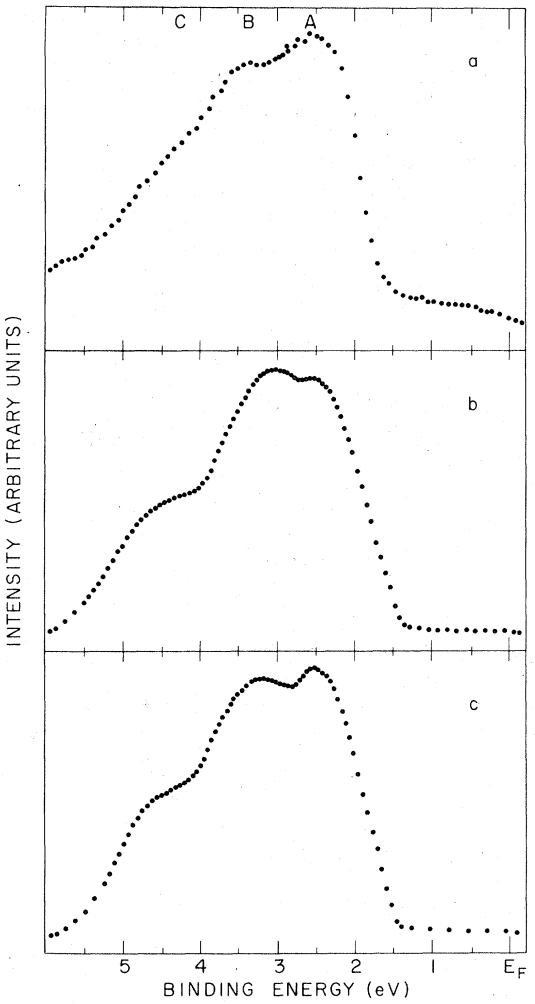

FIG. 1. Densities of electronic states in the valence bands of copper. (a) Polycrystalline Cu XPS spectrum taken from Ref. 4. (b) Predicted density of states based on the formulation and constants used in Ref. 4. (c) Predicted density of states based on the same formulation as (b), but with a different set of modeling constants.

gree in representing the final state. The principal consequence of our work is a *quantitative* appreciation for just where and how the plane wave is inadequate, and the demonstration that single components of APW's can usefully predict high-energy photoemission spectra.

If one is to make meaningful detailed comparisons between theoretical predictions and angle-resolved experiments, we feel that it is essential to have a method which accurately represents the valence-band density of states of the crystal. If this condition is not fulfilled, one should not expect spectra which represent small perturbations on that density of states to agree with theoretical spectral shapes. If good agreement is in fact found, it must be considered a fortuitous cancellation of errors. Unfortunately, in prior calculations, insufficient attention has been given to this important point. The degree of these inaccuracies can be seen in Fig. 1. The experimental spectrum is that of Apai *et al.*[4] of polycrystalline Cu, and as an effectively angle-averaged spectrum should be an accurate representation of the density of states. In comparison to this are the theoretical densities of states used by Wehner *et al.*[3] and Apai *et al.* [curve (b)] and by us [curve (c)] for the calculation of angle-resolved spectra.

Both of these curves have been calculated using the Hodges-Ehrenreich orthogonalized-plane-wave–tight-binding interpolation scheme sampling 308 points in an irreducible $\frac{1}{48}$th of the fcc Brillouin zone. The only difference between the two lies in the choice of the interpolation-scheme parameters. Both of the theoretical spectra have been broadened by 0.8 eV to simulate the experimental spectrum. We note three important features in the experimental density of states. First, a peak labeled A at 2.5 eV binding energy, a second peak B at 3 eV, and an inflection point C at 4.25 eV. It is clear that there are substantial discrepancies between the Hamiltonian of Fig. 1(b) and experiment, particularly in the relative heights of peaks A and B. Experimentally, peak A is the highest point in the spectrum, while this density of states has peak B higher than A. Thus while earlier plane-wave matrix-element calculations predict that for [111] propagation directions the peaks A and B in the angle-resolved spectra should be of equal height, in excellent agreement with experiment, this result should be viewed with some scepticism. This is because the plane-wave matrix elements predict a lowering of the ratio of the intensities of peak B to peak A, while experimentally this ratio is increased. To avoid such ambiguities we have optimized our Hamiltonian to yield a density of states, which is in reasonable quantitative agreement with experiment. The major residual discrepancy is that peak B is still slightly too high with respect to peak A; however, this error is relatively small, and should not preclude a straightforward evaluation of the efficacy of the angle-resolved spectra calculated from it.

In Fig. 2 we compare the results of our APW calculations with the experimental results of Apai *et al.* We also show the results of a plane-wave matrix-element calculation using the same Hamiltonian in order that the two degrees of approximation may be compared. We shall discuss the [111] and [100] experiments in turn.

The [111] experimental geometry gives rise to

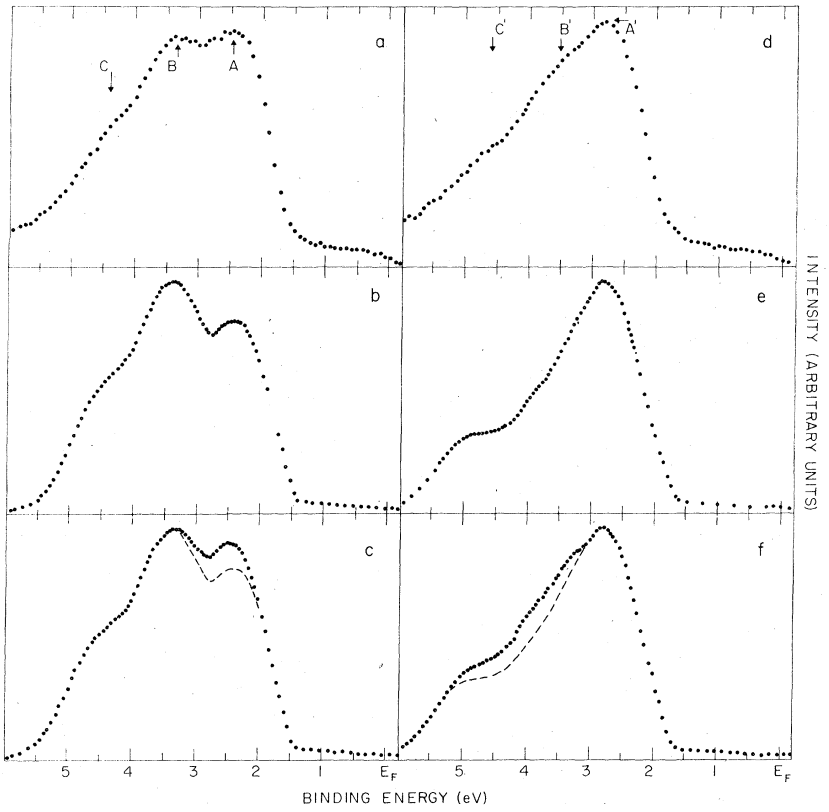

FIG. 2. Comparison of experimental, plane-wave model, and APW-modeled results for Cu. Experimental spectra are taken from Ref. 4. No attempt to simulate conduction-band or secondary-process effects has been made in the calculated spectra. (a)–(c) are, respectively, the experimental, plane-wave, and APW results for spectra along the [111] axis. (d)–(f) are the experimental, plane-wave, and APW results for spectra taken along [001]. The dashed lines in (c) and (f) are rough replicas of the plane-wave results to facilitate comparison.

a spectrum which is rather similar to the polycrystalline spectrum [see Fig. 2(a)]. The principal difference between the two is an increase in the height of peak B relative to peak A in the angle-resolved experiment. With the new Hamiltonian, the plane-wave matrix-element calculation [Fig. 2(b)] successfully predicts this trend, and is still qualitatively in agreement with experiment, although the height of peak B is severely exaggerated. The APW calculation [Fig. 2(c)] clearly is superior in predicting the experimental result. The only significant error of this calculation is that it predicts that peak B should be about 7% higher than peak A, while experimentally they are about equal. Actually, this is about all the accuracy one could expect from this calculation, as the theoretical density of states used also slightly exaggerates the height of peak B relative to peak A as compared to the experimental result. Therefore, accuracy much better than exhibited by Fig. 2(c) would of necessity have been somewhat fortuitous.

As has been previously shown, the plane-wave calculation [Fig. 2(b)] represents the t_{2g} partial density of states of the d band. As is obvious from the disparity, the APW calculation does not. It is equally clear that the two calculations give rather similar results. In fact for this propagation direction, the two are indeed closely related. To see this consider the matrix element A between the state $d_{3z^2-r^2}$ and a final state F:

$$A = \vec{\epsilon} \cdot \langle F | \nabla | d_{3z^2-r^2} \rangle . \tag{15}$$

We break up the integral into three parts,

$$A = \vec{\epsilon} \cdot [2\langle F | \nabla | (z^2/r) F(r) \rangle - \langle F | \nabla | (x^2/r) F(r) \rangle - \langle F | \nabla | (y^2/r) F(r) \rangle] . \tag{16}$$

Since the final state, be it APW or plane wave, is propagating in a direction defined by $x = y = z$, it is clear that the three integrals are equal. Therefore,

$$A = \vec{\epsilon} \cdot (2\alpha\hat{z} - \alpha\hat{x} - \alpha\hat{y}) . \tag{17}$$

In the theory presented by Apai *et al.*, $\vec{\epsilon}$ is at this point effectively assumed to be of the form $\vec{\epsilon} = \hat{x} + \hat{y} + \hat{z}$, yielding

$$A = 2\alpha - \alpha - \alpha = 0 . \tag{18}$$

This describes the "turning off" of this basis function in the [111] direction.

Actually, the proper procedure to follow with Eq. (17) is to square it as it stands and take the averages of the polarization vector components as described in Sec. II. For plane-wave final states, both procedures yield identical results

because $\alpha = 0$. For APW's however, α is a finite number. Thus while the application of the equations of Apai *et al.* to an APW final state would yield a spectrum identical to that obtained in the plane-wave theory, (i.e., a t_{2g} projection), the proper treatment of the electromagnetic field results in differently weighted cross terms in the square of Eq. (17). The effect of these terms is to allow a small, but non-negligible contribution to the spectrum from the e_g states. Based upon our analysis we conclude that due to the nature of the averaging over the orientations of the photon electric vector, it is impossible to eliminate e_g states from the spectra, although they may be strongly suppressed. A pure t_{2g} spectrum could be obtained only by the use of polarized light, with the polarization vector aligned along a $\{111\}$ crystal axis.

In contrast to the case of the [111]-axis experimental geometry, the two calculations for the [100] spectra appear to be quite different. The experimental spectrum [Fig. 2(d)], has basically a one-peaked rather than a two-peaked shape. The highest point in the spectrum, peak A' at 2.9 eV, is shifted in energy from its counterpart peak A in the [111] spectrum by ~0.2 eV. There follows a distinct shoulder B' at 3.65 eV and a more prominent shoulder C' at 4.65 eV. The plane-wave calculation [Fig. 2(e)], as has been found previously for this propagation direction, is notably at variance with the experiment. Here we note that shoulder B' is completely missing from the spectrum and shoulder C' is so exaggerated that the calculation bears little qualitative resemblance to experiment. On the other hand, the APW calculation provides an excellent description of this spectrum. Both shoulders B' and C' occur at the correct energies and have relatively correct shapes. The height of the onset of the shoulder C' is furthermore about half the height of peak A', in agreement with the experiment. This calculation represents the first reasonably successful attempt to describe an ARXPS spectrum of a noble metal for an $\{001\}$ propagation.

There is again a straightforward interpretation of why the plane-wave approximation fails, and why it is so much worse for this experiment than for the [111] direction. The plane-wave calculation predicts that for final-state propagation along the z axis, for example, we have

$$\langle F|\nabla|d_{xy}\rangle = \langle F|\nabla|d_{yz}\rangle = \langle F|\nabla|d_{xz}\rangle = 0 . \qquad (19)$$

For an APW final state, this relation does not hold. This can easily be seen from the matching condition between spherical and plane waves at the APW sphere boundary. A plane wave propagating along the z axis can only be matched onto spherical waves with $m = 0$. Therefore, the d_{xy} matrix element is zero because d_{xy} is composed of $m = \pm 2$ states, and $\Delta m = \pm 2$ transitions are dipole forbidden. The d_{yz} and d_{xz} states, however, are made up of $m = \pm 1$ states, and thus the dipole transitions will be allowed. These states make an important contribution to the spectrum. Further smaller contributions to the spectrum from t_{2g} states arise from polarization averaging effects as in the [111] direction. The fundamental difference is that in this case there is no photon polarization condition that could make the plane-wave result correct.

In fact, if one were to search for an experimental angle of photoemission which maximizes the suppression of t_{2g} orbitals from the spectrum, the [100] axis would not be the best choice. Figure 3 shows the total relative contribution to the d-band spectra for t_{2g} and e_g states for the hypothetical experiment of polarized x rays with $\epsilon = (\hat{x} + \hat{y} + \hat{z})/\sqrt{3}$. This is the physical situation corresponding to the neglect of the photon polarization in the formalism of Apai *et al.* As can be seen from the figure, at a position ~15° from the [001] axis in the direction of [110], the t_{2g} intensity goes to zero. This is a dynamical, rather than a symmetry-based effect, as the position of the zero is a weak function of the ratio of $d \rightarrow p$ to $d \rightarrow f$ radial matrix elements. The zero is due to interference primarily between the ± 3 and ± 1 m_e components of the f channel, which drives the value of the matrix element negative at small angles. The shift in zero comes about through a slight positive shift in value when p contributions are added in. Finally, the radial-matrix-element integral has large contributions only at radii less than 60% of the muffin-tin sphere. Therefore, these matrix elements are insensitive to the wave-function discontinuity at the sphere boundary, and are therefore probably quite accurate. On this basis, we expect that a photoemission spectrum of Cu taken at this angle would be quite similar in appearance to that of Fig. 2(e). The discrepancies between that figure and the proposed experiment would result from photon averaging effects, and would be on the same order of error as that of the [111]-axis plane-wave calculation.

Finally, it is desirable to explain the good results achieved by Wehner *et al.*[3] in their plane-wave calculations. An examination of Fig. 3 shows that all of their spectra, except the [001] direction, were obtained in the region for which the APW and plane-wave d-orbital matrix elements do not grossly differ. If one employed a Hamiltonian accurately representing the valence-band density of states and thereby eliminated those

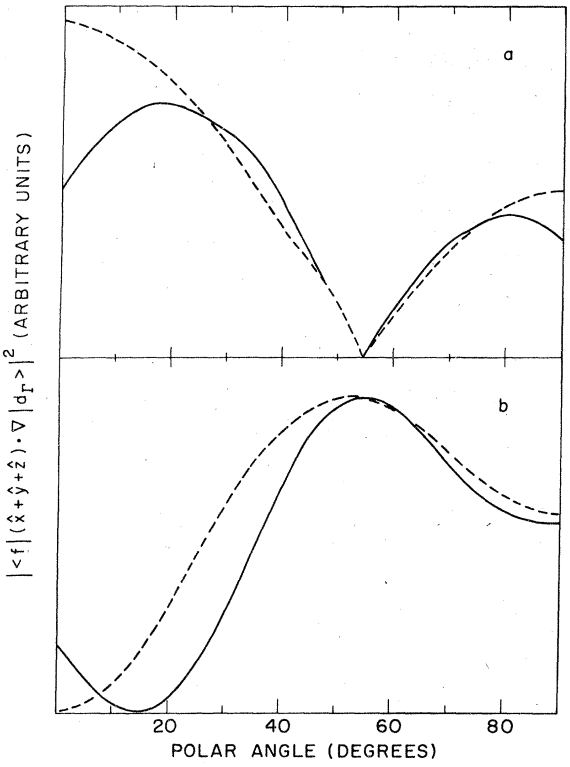

FIG. 3. Comparison of plane-wave (---) and APW (——) matrix elements as functions of polar angle. (a) Shows matrix elements for states transforming under the e_g irreducible representation; (b) serves similarly for the t_{2g} orbitals. These calculations are carried out under the condition that the impinging radiation field is polarized along [111], the consequences of which are explained in the text.

fortuitous cancellations of error remarked upon earlier, one would expect to see the two become basically indistinguishable (in the incorrect polarization formulation) and to see errors in the plane have result relative to the APW calculation, and experiment of the order of those seen in the [111] spectrum.

IV. CONCLUSIONS

In this paper we have developed a statistical model of the high-energy photoemission process. This model requires not only indirect transitions, but also highly mixed final states. This model of the final electronic states implies that even if thermal disorder were minimized by low crystal temperatures, and the fraction of direct transitions became important, the effect on the observed spectral features would be quite small. We have further demonstrated the necessity of including both an accurate representation of the final-state wave function in the core region, and an accurate treatment of the x-ray electromagnetic field. We feel that this approach contains all of the essential physics of these experiments and can be used to predict the outcome of other ARXPS experiments with an accuracy similar to that obtained here. As an additional feature it would be straightforward to include the s-p bands in the calculated spectra, which would probably increase the accuracy of the calculations by smoothing out the slightly excessive modulations that still remain. We have omitted this contribution here only to facilitate a more straightforward comparison with previous work.

Finally, we wish to reemphasize that the model we have developed is valid only in the limit of high photon energy. It would be inappropriate to apply it to ultraviolet-photoemission-spectra experiments at high temperatures, for instance, since the equivalence between intermediate and final states demonstrated in Sec. II for XPS would not obtain, nor would phonon contributions to the momentum of the detected electron be insignificant. The use of single APW matrix elements to describe wave-vector-conserving transitions might also be ill-advised, as in this case, detailed knowledge of the APW expansion coefficients in the final-state wave function would probably be required for accurate results.

ACKNOWLEDGMENTS

We would like to thank Peter Smith for valuable assistance in the calculation of the APW radial matrix elements. Work supported by the Joint Services Electronics Program Contract No. DAAB07-76-C-1400.

[1]R. J. Baird, L. F. Wagner, and C. S. Fadley, Phys. Rev. Lett. 37, 111 (1976).
[2]F. R. McFeely, J. Stöhr, G. Apai, P. S. Wehner, and D. A. Shirley, Phys. Rev. B 14, 3273 (1976).
[3]P. S. Wehner, J. Stöhr, G. Apai, F. R. McFeely, and D. A. Shirley, Phys. Rev. Lett. 38, 169 (1977).
[4]G. Apai, J. Stöhr, R. S. Williams, P. S. Wehner, S. P. Kowalczyk, and D. A. Shirley, Phys. Rev. B 15, 584 (1977).
[5]N. J. Shevchik, Phys. Rev. B 16, 2395 (1977).
[6]R. S. Williams, P. S. Wehner, J. Stöhr, and D. A. Shirley, Phys. Rev. Lett. 39, 302 (1977).
[7]Frederick Wooten, *Optical Properties of Solids* (Academic, New York, 1972).
[8]John M. Ziman, Electrons and Phonons (Oxford U. P., London, 1960).
[9]J. L. Gadzuk, Phys. Rev. B 12, 5608 (1975).
[10]N. J. Shevchik, Phys. Rev. B 16, 3428 (1977).